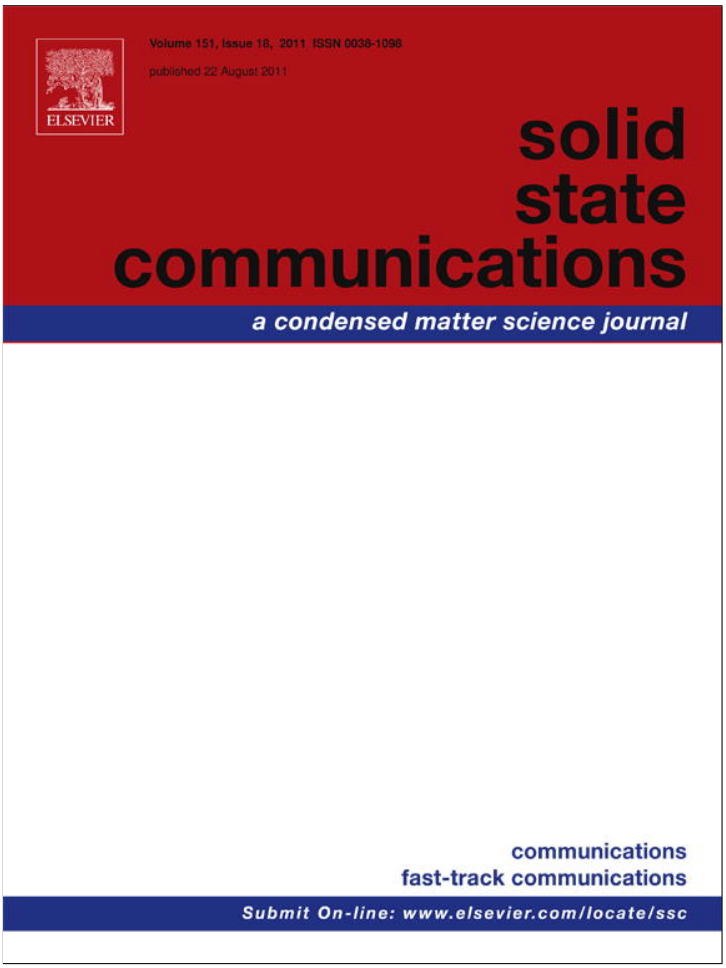

Solid State Communications 151 (2011) 1244–1247

Contents lists available at ScienceDirect

Solid State Communications

journal homepage: www.elsevier.com/locate/ssc

Real-time measurements of sliding friction and elastic properties of ZnO nanowires inside a scanning electron microscope

B. Polyakov [a,c,*], L.M. Dorogin [a], S. Vlassov [a,b], I. Kink [a,b], A. Lohmus [a], A.E. Romanov [a,d], R. Lohmus [a,b]

[a] Institute of Physics, University of Tartu, Riia 142, Tartu, Estonia
[b] Estonian Nanotechnology Competence Centre, Riia 142, 51014, Tartu, Estonia
[c] Institute of Solid State Physics, University of Latvia, Kengaraga 8, Riga, Latvia
[d] Ioffe Physical Technical Institute, RAS, 26 Polytekhnicheskaya, St Petersburg, 194021, Russian Federation

ARTICLE INFO

Article history:
Received 21 March 2011
Accepted 30 May 2011
by C.H.R. Thomsen
Available online 13 June 2011

Keywords:
A. Nanostructures
A. Surfaces and interfaces
C. Scanning and transmission electron microscopy
E. Mechanical properties

ABSTRACT

A real-time nanomanipulation technique inside a scanning electron microscope (SEM) has been used to investigate the elastic and frictional (tribological) properties of zinc oxide nanowires (NWs). A NW was translated over a surface of an oxidised silicon wafer using a nanomanipulator with a glued atomic-force microscopic tip. The shape of the NW elastically deformed during the translation was used to determine the distributed kinetic friction force. The same NW was then positioned half-suspended on edges of trenches cut by a focused ion beam through a silicon wafer. In order to measure Young's modulus, the NW was bent by pushing it at the free end with the tip, and the interaction force corresponding to the visually observed bending angle was measured with a quartz tuning fork force sensor.

1. Introduction

It is well known that the mechanical and electrical properties of single-crystal nanowires (NWs) may be superior in comparison to the corresponding bulk material [1]. Plenty of prototype devices based on NWs have been demonstrated during the last few decades. Individual NWs may be used as sensors, resonance-tunnelling diodes, light-emitting diodes, photodetectors, electromechanical devices and piezoresistors [2–8].

Many methods of investigation of the mechanical properties of either NWs or nanotubes have been developed. Ambient atomic force microscopy (AFM) can be used to vertically load a nanowire suspended over either a hole or a trench to determine Young's modulus and the mechanical strength. This method was applied to Ge NWs and carbon nanotubes (CNTs) [9,10]. The elastic properties and the mechanical strength of SiC NWs and CNTs deposited on a low-friction substrate (MoS_2) and pinned on one end by evaporated metal pads were measured using an AFM lateral force regime [11].

A common way to determine Young's modulus of a NW consists of finding the resonance frequency of a NW fixed from one end and placed inside a scanning electron microscope (SEM) by sweeping the frequency of the external excitation [12]. Another method is based on the lateral bending of the free end of a NW by pushing it with a calibrated contact-mode AFM cantilever, while the NW's second end is fixed on an edge of a rigid substrate. The elastic deformation force is calculated from the visual deformation of the NW and a calibrated AFM cantilever inside the SEM. This method was applied to investigate ZnO NWs [13]. Axial loading or stretching of the NW glued between a rigid substrate and either a calibrated AFM cantilever or between two AFM cantilevers was applied to investigate Si and B NWs, as well as CNTs [14–17]. Analogous axial tensile tests were also performed on ZnO and Si NWs using a MEMS-based nanoscale material testing stage inside a transmission electron microscope (TEM) [18,19]. Real-time force measurement during NW bending was performed by contact-mode AFM inside an SEM to measure Young's modulus of vertically grown arrays of SnO_2 NWs [20].

There are only a few works reporting the measurements of the kinetic friction of a NW on a flat substrate. Manoharan et al. examined the kinetic friction force during the dragging of a ZnO NW parallel to its axis at different loading forces measured by a MEMS-force sensor at ambient conditions [21]. Conache et al. reported the distributed static and kinetic friction of InAs NWs on a Si_3N_4-coated Si wafer based on measuring the curvature of an ultimate NW-bending radius after AFM manipulation in air, where friction was calculated using Young's modulus of a bulk material for calculations [22].

* Corresponding author at: Institute of Physics, University of Tartu, Riia 142, Tartu, Estonia. Tel.: +372 7374723; fax: +372 7383033.
E-mail addresses: celbic@yahoo.com, boriss.polakovs@ut.ee (B. Polyakov).

0038-1098/$ – see front matter © 2011 Elsevier Ltd. All rights reserved.
doi:10.1016/j.ssc.2011.05.045

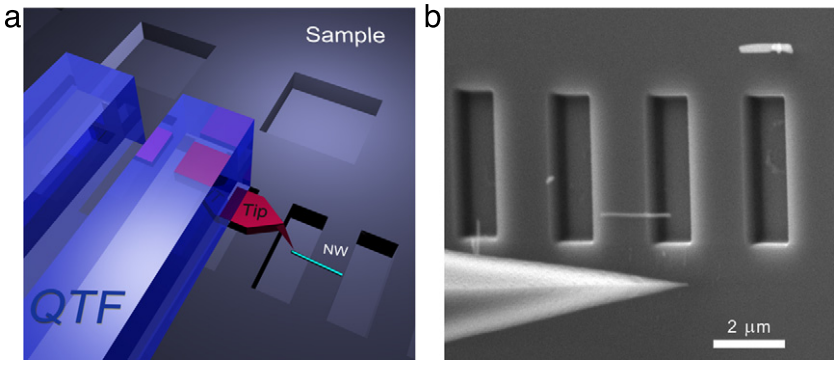

Fig. 1. Schematics of experiment. (a) QTF with the glued AFM tip contacts a NW suspended over a trench on the silicon sample; corresponding SEM image of the AFM tip and FIB cut trenches (b).

In this article, we describe a real-time manipulation technique inside a SEM chamber, which enables the measurement of both the elastic and frictional properties of the same NW on a flat substrate. ZnO NW was translated over a surface of an oxidised silicon wafer using a nanomanipulator equipped with a force sensor composed of a quartz tuning fork (QTF) with a glued AFM tip. The elastic deformation of a translated NW was used to determine the distributed kinetic friction force. The same NW was then positioned half-suspended on edges of trenches cut by a focused ion beam (FIB) on a silicon wafer. To measure the Young's modulus, the free end of the NW was pushed laterally by the AFM tip, and the interaction force corresponding to the visually detected NW bending was measured by a QTF force sensor. No gluing or welding of the NW was performed in these experiments, enabling us to preserve an unchanged NW and making the NW usable for other experiments. Our approach enables us to reduce uncertainties in the measured friction caused by either the use of the bulk value of Young's modulus or the averaged value of the Young's modulus measured on a set of NWs, providing that there is a Young's modulus measured for each particular NW.

2. Experimental

ZnO NWs were grown by a vapour transport method using Au nanoparticles (*BBI international*, 60 nm) as catalysts [23]. NWs were grown on silicon substrates by heating a 1:4 mixture of ZnO and graphite powder to 800–900 °C in an open-end quartz tube for 30 min.

An array of 1 μm-deep trenches sized 3 × 3 μm and 1 × 3 μm was cut by FIB (*FEI* Helios NanoLab) on an Si wafer (50 nm of thermal SiO_2, *University wafers*) (Fig. 1). The wafers were cleaned with RCA-1 solution ("standard clean-1"), followed by 12% HCl, rinsed with distilled water and then blown with nitrogen. The NWs were transferred from the original substrate onto an FIB-patterned wafer surface using a piece of cleanroom paper (Fig. 1(b)).

The tip of the *AdvancedTEC* AFM probes (*Nanosensor* ATEC-CONT cantilevers $C = 0.2$ N/m) used in the experiments was tilted about 15° relative to the cantilever, providing tip visibility from the top. The cantilever was glued with conductive silver epoxy (*Agar Scientific*) to one prong of the QTF (*Elfa*, nominal resonance frequency at 32.768 kHz) forming a force sensor working in the shear oscillating regime (the tip oscillates parallel to the sample surface). To make the QTF response faster, the Q-factor was reasonably decreased by putting a small drop of epoxy resin (Ecobond 286, *Emerson & Cuming*) onto the opposite prong of the QTF. The force constant of cantilevers glued on the QTF was estimated using the Cleveland formula to be 10–20 N/m [24].

The signal from the QTF was amplified by lock-in (SR830, *Stanford Research Systems*) and recorded through the ADC-DAC card (*National Instruments*). The typical values of the driving voltage were 10–30 mV. The force sensitivity of the QTF was calibrated on precalibrated cantilevers (FCL, *AppNano* and CSG11 $C = 0.03$–0.1 N/m, *NT-MDT*) inside the SEM similar to the procedures described in [25,26].

The QTF force sensor was mounted on a 3D nanomanipulator (SLC-1720-S, *SmarAct*) and installed inside the SEM (Vega-II SBU, *TESCAN*) with a typical chamber vacuum of 3×10^{-4} bar. The nanomanipulator enables two types of movement; in the scan regime, the movements are made by either the gradual expansion or contraction of the piezo-nanomanipulator, allowing the force sensor to move smoothly. In the step regime, movements are made in a series of gradual expansions of the piezo-nanomanipulator, followed by abrupt slips achieved via a sawtooth signal sent to the piezo-positioner. Special software was developed to control the nanomanipulator and record simultaneous signals from the nanomanipulator's position sensors and signals from the lock-in amplifier.

We would like to stress some of the advantages of using a QTF with a glued AFM tip as a probe and force sensor compared to the application of a soft AFM cantilever to investigate NW mechanical and frictional properties inside the SEM [13–17]. The QTF provides the real-time data flow of NW-tip interaction with high time and force resolution. Moreover, QTF force sensitivity can be tuned in a wide range by the variation of the applied driving voltage. A high force constant (10–20 N/m) of the AFM cantilever glued to the QTF force sensor enables the easy manipulation of either highly adhered NWs or nanoparticles on the substrate surface [27], which may be problematic if soft AFM cantilevers are used as probes [28].

3. Results and discussion

NWs of suitable lengths (in the order of a few μm) and situated in the proximity of the patterned area were chosen and moved by the AFM tip toward trenches cut by the FIB. To increase loading during the NW translation and to ensure that the tip would not slide over the NW, the force sensor was lowered another 1–2 μm after the tip came into contact with the substrate surface. The oscillation amplitude dropped to zero due to the high repulsive force, and no force measurement was performed during the NW translation.

When the NW is pushed at its midpoint and has travelled over a few microns, it bends into an arc due to the distributed kinetic friction force acting along the NW's length (Fig. 2). The NW's characteristic shape remains constant during the translation due to the fact that the total kinetic friction force acting on the NW is balanced with the external force applied by the tip. The determination of the distributed kinetic friction for too-short NWs was problematic due to the large radius of the curvature during the translation. The minimal length suitable for the determination of kinetic friction depends on the NW's diameter, and was usually at least 2 μm in our experiments.

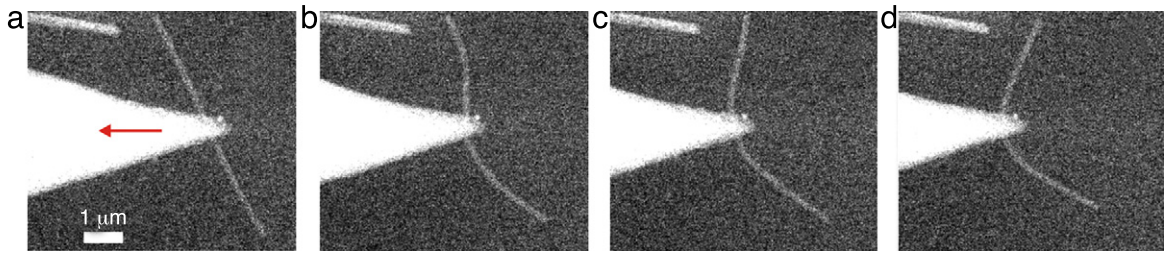

Fig. 2. Evolution of the NW shape profile during the NW dragging. AFM tip contacts the intact NW, the arrow indicates the direction of tip movement (a); Partially displaced NW (b); Completely displaced NW (c); Final characteristic shape (d).

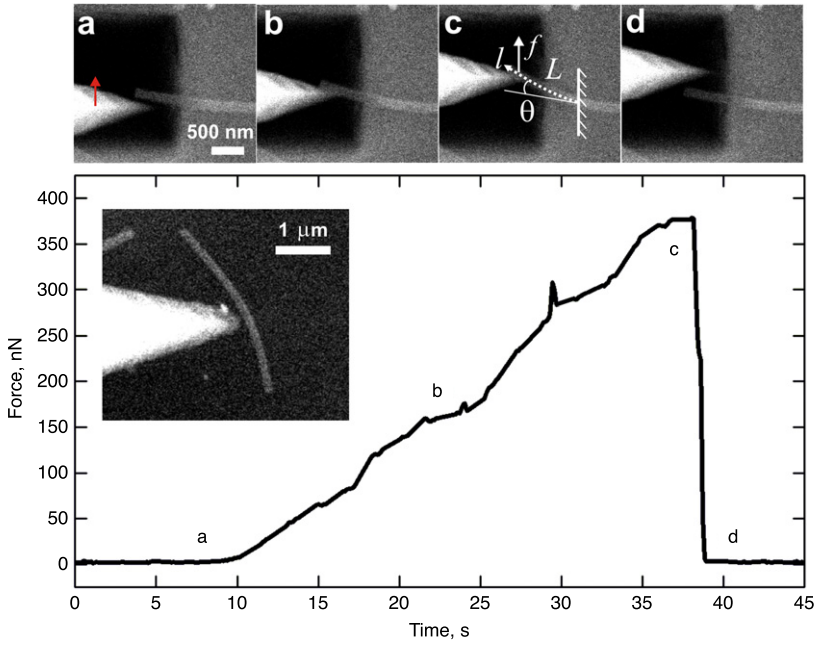

Fig. 3. SEM images of the suspended NW being pushed by the tip and the corresponding force curve. The tip approaches the NW, the arrow indicates the direction of tip movement (a), the NW is slightly bent (b), maximal bending of NW and the corresponding schematics of the NW loading laid over the SEM image; the natural axis l, the angle θ between the tangent of the bent NW profile projected on an initial NW profile, the length L of the suspended part of the NW and the applied force f are shown (c), the NW has come off the tip and the force has dropped to zero (d). Inset: The characteristic shape of the same NW dragged by the tip over the sample surface before it has been positioned on the trench edge. The calculated Young's modulus and the friction force are $E = 58$ GPa and $q_{kin} = 0.14$ nN/nm, respectively.

Table 1
Kinetic friction and Young's modulus of ZnO NW.

Nr.	Diameter, nm	Length, nm	q_{kin}, nN/nm	σ_{kin}, MPa	Young's modulus, GPa
1	112	3850	0.115	1.8	38
2	125	3280	0.135	1.9	58
3	160	3140	0.2	2.2	27
4	180	4640	0.25	2.4	41
5	230	4615	0.3	2.3	38

We applied the Timoshenko beam theory to calculate the NW bending profile during its translation with the method described in [29]. Considering the NW length L, diameter D, a measured Young's modulus of E and the NW profile shape experimentally obtained from the SEM image, one can estimate the distributed kinetic friction force as q_{kin} (the Young's modulus measurement procedure will be described below). Measurements were performed on five NWs with different diameters. Interfacial shear stress σ_{kin}, which is considered to be a fundamental property of nanoscale friction, can be calculated assuming a hexagonal cross-section of NWs as $\sigma_{kin} = q_{kin}\sqrt{3}/D$ [30]. The results are presented in Table 1. The average value of the interfacial shear stress is $\sigma_{kin} = 2.1 \pm 0.26$ MPa. Our results are in good agreement with the 1 MPa value of the interfacial shear stress obtained by Manoharan et al. for ZnO 30–40 μm-long NWs with 200 nm diameters parallel to the NW axis dragging [21].

To determine the Young's modulus of the NWs, the NWs were positioned on the edges of the cut trenches of the FIB as shown in Figs. 1 and 3. One end of the NW was suspended over the trench, and another end was kept fixed to the substrate surface by a strong adhesion force. The suspended part of the NW was pushed by the AFM tip during the continuous movement of the manipulator (the scan regime) parallel to the trench wall (Fig. 3). The QTF oscillation amplitude signal (which directly correlates with the applied force) and the grabbed SEM images were recorded simultaneously during the experiment. In our experiment, the length of the suspended part of NW was about 1 μm in contrast to at least a few tens of μm in other works dealing with NW bending [13,31]. This method gives us the possibility to measure Young's modulus of rather short NWs with lengths of a few microns.

Worth noting is that the region close to the trench (approximately 250–500 nm) is slightly concave due to an imperfect focus-

ing of the ion beam. That causes an increase of length of the NW's suspended part L (shifted to the right relative to the trench wall). The suspended part of the NW looks more transparent in comparison to the adhered part (Fig. 3(a)–(d)).

The equation of the equilibrium for a bent elastic beam with Young's modulus E and I momentum of inertia being loaded by a point force f at its end can be written as [32,33]:

$$E \cdot I \cdot \frac{\mathrm{d}^2\theta}{\mathrm{d}l^2} + f \cdot \cos\theta = 0, \tag{1}$$

where l is the natural axis of the NW, θ is the angle between the tangent of the bent NW profile projected on an initial NW profile and L is the length of the suspended part of the NW. The equation can either be solved numerically or expressed in elliptic functions with the boundary conditions:

$$\theta|_{l=0} = 0 \tag{2a}$$

$$\left.\frac{\mathrm{d}\theta}{\mathrm{d}l}\right|_{l=L} = 0. \tag{2b}$$

Eq. (2a) implies that the NW is fixed along its axis in the adhered part, and Eq. (2b) is dictated by the absence of momentum at the end of the NW. To process data in order to find the value of Young's modulus, an SEM image of the NW profile was numerically fitted to the curve given by Eq. (1).

The typical force curve and the corresponding SEM images are presented in Fig. 3. Young's modulus for this wire was found to be 58 GPa. The characteristic shape of the NW during the dragging before it had been positioned on the edge of the trench is shown in the inset. The distributed friction force and the kinetic friction shear stress were found to be 0.14 nN/nm and 1.9 MPa, respectively.

We found the averaged value of Young's modulus to be 40.4 ± 11 GPa (Table 1). The mean value is in good agreement with other works performed on ZnO NWs; Manoharan et al. found 40 GPa for a NW with a diameter of 200–750 nm [13] and Song et al. found 29 GPa for a NW with a diameter of 45 nm [34].

Significant variation in magnitudes of Young's modulus from 27 to 58 GPa in the measured set of NWs makes it important to gather the Young's modulus for each NW individually evident in order to obtain calculations of kinetic friction based on the balance of elastic and friction forces. Variation in sliding friction and shear stress values was of the order of magnitude for InAs NWs [22], probably due to the usage of the bulk modulus of InAs in such calculations. In our experiment the standard error was about 12% of the mean value of kinetic shear stress. Thus, the use of individual values of Young's modulus is able to make friction force and shear stress determination more reliable.

In most bending experiments, the adhered part of the NW remained motionless. It means that the applied force was lower than the static friction force between the NW and the substrate. NWs were never broken during the bending experiment, even at large bending angles ($\theta \approx 60°$). In a few cases, NWs were broken by the tip in an abrupt motion (step regime), when the tip was close to a trench wall. We avoided positioning the tip closer to the trench wall due to the risk of touching the wall and introducing artifacts to the force curve.

It was possible to displace as a whole only NWs having a high Young's modulus and/or a very short part adhered to the substrate. The NW with a full length 4500 nm and adhered part $l = 550$ nm was displaced, when the maximal force of $F = 1620$ nN was detected. This force corresponds to the averaged static friction force $q_{st} = F/l = 3$ nN/nm. In our previous work, we found the averaged static friction force of ZnO NW on a Si wafer to be about 2.2 nN/nm when it was measured by another method [29]. Our approach opens a route to measure Young's modulus of a NW and then to find the maximal static friction force. This can be done for a NW having adhered part long enough to keep the NW fixed to the substrate via sequential shortening the adhered part of the NW by FIB followed by pushing the NW with an AFM tip until the whole NW is displaced.

4. Conclusions

In this work, we presented a novel method to determine the elastic and frictional properties of the same NW. Distributed kinetic friction and corresponding interfacial shear stress were calculated from the characteristic shape of NW bending during the translation on a flat substrate performed by an AFM tip glued on the QTF. Distributed kinetic friction q_{kin} and interfacial shear stress σ_{kin} of a ZnO NW on an oxidised Si substrate were found to be 0.2 ± 0.08 nN/nm and 2.1 ± 0.26 MPa, respectively. Young's modulus was measured for the same set of NWs by bending its half-suspended part and was found to be 40.4 ± 11 GPa.

Acknowledgments

This work was supported by the Estonian Science Foundation grants no. 8377, 8420 and JD162, the Estonian research targeted project SF0180058s07, the Doctoral School of Functional Materials and Technology, the University of Tartu, the Estonian Nanotechnology Competence Centre and the ESF Fanas program "Nanoparma".

References

[1] Z. Wang (Ed.), Nanowires and Nanobelts: Materials, Properties and Devices, first ed., in: Metal and Semiconductor Nanowires, vol. 1, Springer, USA, 2005.
[2] A. Kolmakov, Y. Zhang, G. Cheng, M. Moskovits, Adv. Mater. 15 (2003) 997–1000.
[3] L. Samuelson, M. Bjork, K. Deppert, M. Larsson, B. Ohlsson, N. Panev, A. Persson, N. Skold, C. Thelander, L. Wallenberg, Physica E 21 (2004) 560–567.
[4] C. Soci, A. Zhang, B. Xiang, S. Dayeh, D. Aplin, J. Park, X. Bao, Y.H. Lo, D. Wang, Nano Lett. 7 (2007) 1003–1009.
[5] M. Gudiksen, L. Lauhon, J. Wang, D. Smith, C. Lieber, Nature 415 (2002) 617–620.
[6] K. Ziegler, D. Lyons, J. Holmes, D. Erts, B. Polyakov, H. Olin, K. Svensson, E. Olsson, Appl. Phys. Lett. 84 (2004) 4074–4076.
[7] Z. Wang, Adv. Funct. Mater. 18 (2008) 3553–3567.
[8] K. Liu, P. Gao, Z. Xu, X. Bai, E. Wang, Appl. Phys. Lett. 92 (2008) 213105.
[9] J. Salvetat, J. Bonard, N. Thomson, A. Kulik, L. Forro, W. Benoit, L. Zuppiroli, Appl. Phys. A 69 (1999) 255–260.
[10] L. Ngo, D. Almecija, J. Sader, B. Daly, N. Petkov, J. Holmes, D. Erts, J. Boland, Nano Lett. 6 (2006) 2964–2968.
[11] E. Wong, P. Sheehan, C. Lieber, Science 277 (1997) 1971–1975.
[12] Y. Huang, X. Bai, Y. Zhang, J. Phys.: Condens. Matter 18 (2006) L179–L184.
[13] M. Manoharan, A. Desai, G. Neely, M. Haque, J. Nanomater. (2008) Article ID 849745.
[14] M. Yu, B. Files, S. Arepalli, R. Ruoff, Phys. Rev. Lett. 84 (2000) 5552–5555.
[15] Y. Zhu, F. Xu, Q. Qin, W. Fung, W. Lu, Nano Lett. 9 (2009) 3934–3939.
[16] C. Hsin, W. Mai, Y. Gu, Y. Gao, C. Huang, Y. Liu, L. Chen, Z. Wang, Adv. Mater. 20 (2008) 3919–3923.
[17] C. Lin, H. Ni, X. Wang, M. Chang, Y. Chao, J. Deka, X. Li, Small 6 (2010) 927–931.
[18] R. Agrawal, B. Peng, H. Espinosa, Nano Lett. 9 (2009) 4177–4183.
[19] A. Lugstein, M. Steinmair, A. Steiger, H. Kosina, E. Bertagnolli, Nano Lett. 10 (2010) 3204–3208.
[20] S. Barth, C. Harnagea, S. Mathur, F. Rosei, Nanotechnology 20 (2009) 115705.
[21] M. Manoharan, M. Haque, J. Phys. D: Appl. Phys. 42 (2009) 095304.
[22] G. Conache, S. Gray, A. Ribayrol, L. Froberg, L. Samuelson, H. Pettersson, L. Montelius, Small 5 (2009) 203–207.
[23] M. Huang, Y. Wu, H. Feick, N. Tran, E. Weber, P. Yang, Adv. Mater. 13 (2001) 113–116.
[24] C. Gibson, D. Smith, C. Roberts, Nanotechnology 16 (2005) 234–238.
[25] C. Su, L. Huang, K. Kjoller, Ultramicroscopy 100 (2004) 233–239.
[26] S. Fain Jr., K. Barry, M. Bush, B. Pittenger, R. Louie, Appl. Phys. Lett. 76 (2000) 930.
[27] S. Vlassov, B. Polyakov, L.M. Dorogin, A. Lõhmus, A.E. Romanov, I. Kink, E. Gnecco, R. Lõhmus, Solid State Commun 151 (2011) 688–692.
[28] R. Resch, A. Bugacov, C. Baur, B. Koel, A. Madhukar, A. Requicha, P. Will, Appl. Phys. A 67 (1998) 265–271.
[29] B. Polyakov, L. Dorogin, A. Lohmus, A. Romanov, R. Lohmus, Manuscript.
[30] M. Bordag, A. Ribayrol, G. Conache, L. Froberg, S. Gray, L. Samuelson, L. Montelius, H. Pettersson, Small 3 (2007) 1398–1401.
[31] A. Desai, M. Haque, Appl. Phys. Lett. 90 (2007) 033102.
[32] S. Timoshenko, J. Goodier, Theory of Elasticity, second ed., McGraw-Hill Book Company, New York, 1951, pp. 316–342.
[33] L. Landau, E. Lifshitz, Theory of Elasticity, third ed., vol. 7, Butterworth-Heinemann, Oxford, 1986.
[34] J. Song, X. Wang, E. Riedo, Z. Wang, Nano Lett. 5 (2005) 1954–1958.